

Intensification of *Reutealis trisperma* biodiesel production using infrared radiation: Simulation, optimisation and validation



A.S. Silitonga^{a, b, *}, T.M.I. Mahlia^{b, c}, F. Kusumo^d, S. Dharma^a, A.H. Sebayang^a,
R.W. Sembiring^e, A.H. Shamsuddin^f

^a Department of Mechanical Engineering, Politeknik Negeri Medan, 20155 Medan, Indonesia

^b Department of Mechanical Engineering, College of Engineering, Universiti Tenaga Nasional, 43000 Kajang, Selangor, Malaysia

^c School of Systems, Management and Leadership, Faculty of Engineering and Information Technology, University of Technology Sydney, NSW 2007, Australia

^d Department of Computer Science & Information Technology, College of Computer Science & Information Technology Universiti Tenaga Nasional, 43000 Kajang, Selangor, Malaysia

^e Department of Computer and Information Engineering, Politeknik Negeri Medan, 20155 Medan, Indonesia

^f Institute of Sustainable Energy, Universiti Tenaga Nasional, 43000 Kajang, Selangor, Malaysia

ARTICLE INFO

Article history:

Received 13 December 2017

Received in revised form

11 September 2018

Accepted 5 October 2018

Available online 12 October 2018

Keywords:

Reutealis trisperma biodiesel

Transesterification

Infrared radiation

Response surface methodology

Box-behnken design

ABSTRACT

Biodiesel production using intensification of methyl ester is becoming very important due to its considerably lower energy requirement and shorter reaction time in obtaining feedstock oil. The present study investigated utilisation of *Reutealis trisperma* oil to produce biodiesel. A Box-Behnken experimental design was used to optimise the transesterification process. The process variables were explored and the optimum methanol to oil molar ratio, catalyst concentration, reaction temperature, and reaction time were 8:1, 1.2 wt%, 64 °C and 68 min respectively and the corresponding methyl ester yield was 98.39%. The experiment was conducted in triplicate to validate the quadratic model. Results showed average methyl ester yield was 97.78%, which is close to the predicted value, indicating reliability of the model. Results also indicated that using infrared radiation method has many advantageous, such as less energy consumption as a result of deeper penetration of reactant mass which can improve mass transfer between the immiscible reactants in order to improve quality of biodiesel. The physicochemical properties of *Reutealis trisperma* methyl ester produced under optimum transesterification process variables were also measured and the properties fulfilled the fuel specifications as per ASTM D6751 and EN 14214 standards.

© 2018 Elsevier Ltd. All rights reserved.

1. Introduction

Fossil fuels, such as petroleum, gasoline and diesel are important in meeting the energy demands of the transport sector. However, since these are non-renewable energy sources, it is forecasted petroleum will be exhausted completely in 2055 based on estimated “proven fossil fuel reserves”, which are essentially reserves where petroleum can be extracted using existing fuel processing technologies [1,2]. In fact, it is very likely that petroleum will be exhausted sooner than expected if the global energy demands increase at a pace that exceeds the availability of fossil fuel

reserves. For this reason, the scientific community has focused efforts to introduce alternative fuels from renewable sources. Biodiesels are among the most attractive alternative fuels to fulfil these global energy demands and needs. These fuels have a great potential as diesel substitutes because they can be specially formulated to contain physicochemical properties, cold flow properties, and oxidation stability comparable with those of diesel [3,4]. Additionally, it has been proven burning of biodiesels produce lower emissions [5].

There are three types of biodiesels: (1) first-generation biodiesels (biodiesels produced from edible vegetable oils), (2) second-generation biodiesels (biodiesels produced from non-edible vegetable oils), and (3) third-generation biodiesels (biodiesels produced from macroalgae and microalgae-derived oils) [6–8]. Various non-edible vegetable oils have been explored for

* Corresponding author. Department of Mechanical Engineering, Politeknik Negeri Medan, 20155 Medan, Indonesia.

E-mail addresses: arridina@polmed.ac.id, ardinsu@yahoo.co.id (A.S. Silitonga).

biodiesel production in order to reduce human dependency on edible oils for fuel production. As the name implies, these vegetable oils are called “non-edible oils” as they are unfit for human consumption owing to their toxicity [9,10]. Hence, these oils have gained popularity, especially in developing countries, in order to resolve the “food versus fuel” dilemma. However, it is well known non-edible oils have high levels of free fatty acids, which leads to significant saponification during the alkaline-catalysed transesterification.

Reutealis trisperma (commonly known as Philippine Tung) is native to the Philippines. It belongs to the family of Euphorbiaceae and found throughout Southeast Asia. The annual yield of *reutealis trisperma* seed oil is 400 kg/ha [11,12] while its kernel oil yield is between 45% and 50%. Reddish yellow in colour, the oil is considered toxic to humans and animals due to its high amount of naturally present alpha-eleostearic acid [11,13]. The *Reutealis trisperma* plant helps to prevent land erosion and is an excellent producer of oxygen [14].

Biodiesel production has also focused on utilising existing technologies, such as radiation, cavitation and oscillatory flow among others. These technologies can produce high methyl ester yields as well as improve the quality of biodiesel through enhancement of mass and heat transfer in the reactor [5,9]. Holilah et al., [15] showed the optimum reaction condition for biodiesel production from *Reutealis trisperma* which can provide a maximum yield of 95.15%. Sarifah Nurjanah et al., [16] reported esterification and transesterification for biodiesel production *Reutealis trisperma* produced highest yield of FAME 61.1%. This production process has a longer reaction time and produce lower methyl ester yields [17,18]. Therefore, several methods have been studied in recent years such as, non-catalytic supercritical, microwave, ultrasound-assisted, and infrared radiation techniques to produce biodiesel [19–21]. Among them, the infrared energy within a range of 0.001–1.7 eV can penetrate through the reactants mass at deeper depths [22]. These technologies can be used to intensify biodiesel production by enhancing heat and mass transfer of the reactants which will in turn maximise biodiesel yield [23]. This method has been proven to reduce both reaction time and energy consumption in order to improve the quality biodiesel compared with conventional heating systems [22]. Chakraborty and Sahu reported that infrared radiation-assisted reactor was sufficiently effective, required less time, and produced higher ester yield compared with the conventional method using waste goat tallow [19]. Indeed, one study has shown that the production of biodiesel from transesterification of waste mustard oil through infrared radiation is energy-efficient [9].

In this study, a different approach was used to maximise the yield of *Reutealis trisperma* biodiesel to produce biodiesel on a commercial scale. In order to reduce fatty acid content of the RTO, acid-catalysed esterification and alkaline-catalysed transesterification was carried out with the aim to produce *Reutealis trisperma* methyl ester (RTME). The uniqueness of this study is both of these processes were intensified using infrared radiation. In addition, unlike other researches (which focused on optimising the process variables of acid-catalysed esterification), the present study focused on optimising the process variables (in particular, the methanol to oil molar ratio, KOH catalyst concentration, reaction temperature, and reaction time) of the infrared radiation-assisted transesterification process. Response surface methodology (RSM) based on the Box-Behnken experimental design was used for this purpose. The RSM enables one to optimise the process variables and to visualise the interaction effects of the process variables on the RTME yield using three-dimensional response surface plots. It is believed that the approach discussed in this paper will be of great interest to scientists and researchers, especially those who intend

to maximise biodiesel yields produced from non-edible oil feedstocks with high free fatty acid content in an efficient and effective manner.

2. Materials and methods

2.1. Materials

The RTO was purchased from Koperasi Lestari, Cilacap, Java, Indonesia. It was degummed and filtered for biodiesel production. The following reagents used for biodiesel production were sourced from It Tech Research (M) Sdn. Bhd., Malaysia: (1) methanol (purity: 99.9%, grade: ACS reagent), (2) sulfuric acid (purity: >98.9%), (3) anhydrous sodium sulphate (purity: 99%), (4) potassium hydroxide pellets (purity: 99%), (5) fatty acid methyl ester (FAME) mix, C₈–C₂₄, (brand: Sigma-Aldrich, packaging size: 100 mg), (6) methyl nonadecanoate, C₁₉ (brand: Sigma-Aldrich, purity: >99.5%) (7) 1,2,4-butanetriol, (8) glyceryl mononadecanoate, mono C₁₉, (9) glyceryl dinadecanoate, di C₃₈, (10) glyceryl tridonadecanoate, tri C₅₇, and (11) Fluka® Analytical phenolphthalein solution (1% in ethanol).

2.2. Experimental setup

The infrared radiation-assisted reactor consisted of a 500-mL transparent borosilicate glass (CSL-1380 unjacketed with 5 mm thickness) fitted with an infrared lamp (input power: 100 W, mains voltage: 220 V, mains frequency: 50 Hz) in order to generate infrared energy within a range of 0.001–1.7 eV. The 100 W infrared lamp was placed in front of the 500-mL glass reactor connected to an overhead stirrer fitted with a digital speed indicator and the stirring speed was set at 1000 rpm. The overhead stirrer was used to ensure homogeneous mixing of the reaction mixture in the reactor. The schematic diagram of the experimental setup used for infrared radiation-assisted biodiesel synthesis is shown in Fig. 1. It should be noted this experimental setup was used for both acid-catalysed esterification and alkaline-catalysed transesterification.

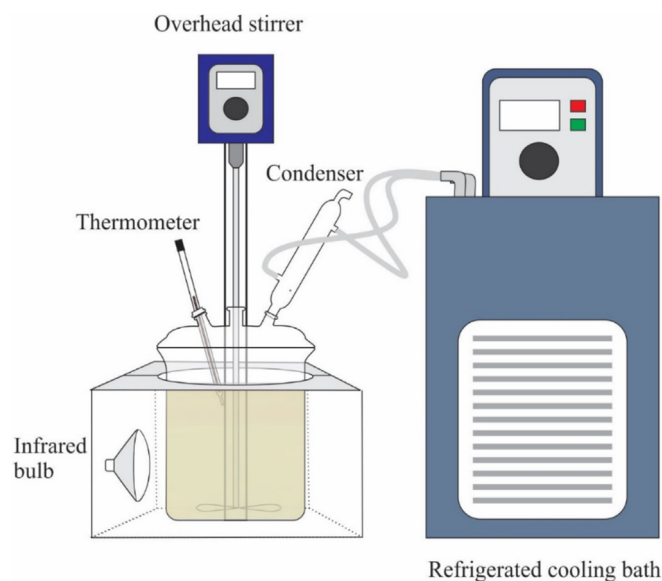


Fig. 1. Schematic diagram of infrared radiation-assisted reactor used for esterification and transesterification of RTO.

2.3. Infrared radiation-assisted acid-catalysed esterification and alkaline-catalysed transesterification

It was necessary to perform pre-treatment of the RTO in order to reduce its free fatty acid content (and thus, its acid value) prior to the transesterification process. Acid-catalysed esterification was used for this purpose where acids such as H_2SO_4 were used as the catalyst [24]. In this study, infrared radiation-assisted acid-catalysed esterification process was carried out where 2 vol% of H_2SO_4 was added into 500 mL of crude RTO at 65 °C. The methanol to oil molar ratio and stirring speed were kept fixed at 8:1 and 1000 rpm respectively. However, the reaction time was varied at 30, 60, 90, 120, and 150 min to examine their effects on the acid value of the esterified *Reutealis trisperma* oil (ERTO). When the esterification reaction was completed, ERTO was poured into a different funnels to separate ERTO from methanol and other impurities. Once the separation process was over, there were two distinct layers in the separating funnel - the top layer consisted of methanol and other impurities while the bottom layer consisted of ERTO.

Following this, infrared radiation-assisted alkaline-catalysed transesterification process was carried out where KOH was used as the catalyst and it was diluted into methanol. The KOH-methanol mixture was later added into the ERTO. The stirring speed was kept fixed at 1000 rpm and the reaction time varied between 60 min and 120 min. Once the transesterification reaction was complete, the reaction mixture was left to stand overnight in the separating funnel in order to separate glycerol and other impurities from RTME by gravity. Similar to ERTO, two distinct layers were formed in the separating funnel after the separation process. The top layer consisted of RTME whereas the bottom layer consisted of a mixture of glycerol and other impurities drained from the separating funnel. The RTME (biodiesel) was washed with warm water several times and then poured into a vacuum evaporator set at 60 °C to remove moisture and unreacted methanol.

2.4. Optimisation of the infrared radiation-assisted alkaline-catalysed transesterification process variables using RSM

Design-Expert[®] Version 9.0.6.2 software was used to optimise the process variables of the transesterification process while the Box-Behnken experimental design was used to optimise the methanol to oil molar ratio (x_1), KOH catalyst concentration (x_2), reaction temperature (x_3), and reaction time (x_4) in order to maximise RTME yield. It should be noted here the process variables are independent, whereas RTME yield is the dependent variable or response variable. The RSM was used to examine the interaction effects of the process variables on RTME yield.

2.5. Physicochemical properties and FAME content of RTME produced from infrared radiation-assisted alkaline-catalysed transesterification with optimum process variables

The optimum process variables of the alkaline-catalysed transesterification process were intensified using infrared radiation (methanol to oil molar ratio, KOH catalyst concentration, reaction temperature, and reaction time) determined from RSM were used to produce the RTME.

The FAME content of the RTME was determined using gas chromatography based on EN14103:2011 standard test method. The gas chromatograph was equipped with a flame ionisation detector to determine the FAME content and linolenic acid methyl ester ($C_{18:3}$) content of biodiesels. According to the EN14103:2011 standard test method, FAME content of the biodiesel should be more than 90 wt%, while the linolenic acid methyl acid content should be within the range of 1–15 wt%, consistent with the EN

14214 fuel specifications. This method is suitable for biodiesels that contain methyl esters C_6 and C_{24} . The gas chromatograph is equipped with an Agilent HP-INNOWax high polarity column (length \times inner diameter \times film thickness: 30 m \times 0.25 mm \times 0.25 μ m, stationary phase: polyethylene glycol). In this study, helium was used as the carrier gas and the operating conditions of the gas chromatography measurements are shown in Table 1. The FAME content of the RTME was determined using Eq. (1) whereas the linolenic acid methyl ester content was determined using Eq. (2).

$$FAME = \frac{\sum A - A_{EI}}{A_{EI}} \times \frac{W_{EI}}{W} \times 100 \quad (1)$$

$$L = \frac{A_L}{A_{EI}} \times \frac{W_{EI}}{W} \times 100 \quad (2)$$

Here, FAME represents the content in percent by weight (wt%), $\sum A$ is the total peak area from FAME C_6 and C_{24} , A_{EI} is the peak area corresponding to methyl nonadecanoate (methyl ester C_{19}), W_{EI} is the weight of methyl nonadecanoate (methyl ester C_{19}) in milligrams (mg), which is used as the internal standard, W is the weight of the sample in milligrams (mg), L represents the linolenic acid methyl ester content in percent by weight (wt%), and A_L is the peak area corresponding to the linolenic acid methyl ester.

3. Results and discussion

3.1. Effect of reaction time on acid value of ERTO produced from infrared radiation-assisted acid-catalysed esterification process

Fig. 2 shows the effect of reaction time (30–150 min) on acid value of ERTO obtained from the infrared radiation-assisted acid-catalysed esterification process. It can be seen the acid value of the ERTO was highest at a reaction time of 30 min, whereas the acid value of the ERTO was lowest (2.25 mg KOH/g) at a reaction time of 90 min. However, it is interesting to note there was a slight increase in the acid value when the reaction time was further increased after 90 min, which was due to undesirable side reactions in the presence of the H_2SO_4 catalyst. Based on the results, the ERTO with the lowest acid value was chosen for the infrared radiation-assisted alkaline-catalysed transesterification.

3.2. Optimisation of the infrared radiation-assisted alkaline-catalysed transesterification process variables using RSM

The RSM based on the Box-Behnken experimental design was used to optimise the process variables of the infrared radiation-assisted alkaline-catalysed transesterification in order to maximise RTME yield. With four factors and three levels for each factor, the experimental design consisted of 29 experiments. The experimental RTME yield for each combination of methanol to oil molar ratio, KOH catalyst concentration, reaction temperature, and reaction time was determined for each experiment, as shown in Table 2.

The response surface quadratic model used to predict the RTME yield is given by Ref. [15]:

$$Y = \beta_0 + \sum_{j=1}^n \beta_j \beta_j + \sum_{j=1}^n \beta_{jj} \beta_j^2 + \sum_{i=1}^{j-1} \sum_{j=2}^n \beta_{ij} x_i x_j + \varepsilon \quad (3)$$

where Y is the RTME yield (response variable), β_0 , β_i , β_j , and β_{ij} represent the regression coefficients of the independent variables for the intercept, linear, quadratic, and product terms, respectively, x_i and x_j are the uncoded independent variables, and n is the

Table 1
Operating conditions for gas chromatography measurements according to EN 14103:2011 standard test method.

Parameters	Specification
Capillary column	Agilent HP-INNOWax column
Oven temperature	Length × inner diameter × film thickness: 30 m × 0.25 mm × 0.25 μm 60 °C for 2 min 60–200 °C at 10 °C/min 200–240 °C at 5 °C/min 240 °C for 7 min Post-run at 255 °C for 0.5 min
Carrier gas	Helium
Helium pressure	70 kPa
Flow rate	1.5 mL/min
Split flow	100 mL/min
Split injection ratio	100:1.5
Injector temperature	250 °C
Detector temperature	250 °C
Type of injector	Split/Splitless
Type of detector	Flame ionisation detector
Injection volume	1 μL
Flame ionisation detector makeup gas	Nitrogen
FAME standard	FAME mix C ₈ –C ₂₄ , Brand: Sigma-Aldrich, Packaging size: 100 mg

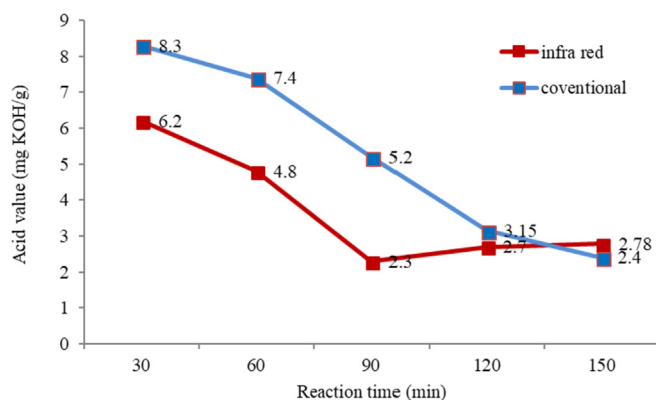


Fig. 2. Effect of reaction time on the acid value of the ERTO.

number of factors optimised in the experiment. In this study, $n = 4$ because four process variables are optimised for the infrared radiation-assisted alkaline-catalysed transesterification process.

Hence, Eq. (3) can be rewritten as:

$$\begin{aligned}
 Y = & -306.08667 + 46.17792x_1 + 81.35833x_2 + 1.99683x_3 \\
 & + 2.09158x_4 + 0.035x_1x_2 + 0.17x_1x_3 + 0.033958x_1x_4 \\
 & - 0.0663x_2x_3 - 184x_2x_4 - 0.0027667x_3x_4 - 3.43510x_1^2 \\
 & - 12.50167x_2^2 - 0.014217x_3^2 - 0.014x_4^2
 \end{aligned}
 \quad (4)$$

Eq. (4) represents the response surface quadratic model used to predict RTME yield as a function of transesterification process variables (uncoded independent variables). The RTME yield values predicted using this model are shown in Table 3. It can be seen that there is good agreement between RTME yield predicted using the response surface quadratic model and RTME yield obtained from the Box-Behnken experimental design.

Analysis of variance (ANOVA) was used to determine the reliability of the response surface quadratic model and the results are summarised in Table 3. The model is considered as significant if the computed F -value is greater than the critical F -value. It can be seen that the F -value of the model is 84.89, which is greater than the critical F -value ($F_{0.05(14,14)} = 2.48$), indicating the model is significant. In addition, the probability of a large F -value (Prob. > F) of the

model is less than 0.0001, indicating there is less than 0.01% chance that the large F -value is because of random errors. The lack of fit F -value of the model is 3.20, which is not significant relative to the pure error. In addition, the lack of fit F -value of the model is less than the critical F -value ($F_{0.05(10,5)} = 5.96$), indicating the model fits well with the experimental data. The coefficient of determination (R^2) was found to be 0.9884, indicating 98.84% of the variability of RTME yield is due to the process variables while the rest is not described by the model. In general, R^2 value (0.9884) is close to the adjusted R^2 value (0.9767), indicating the response surface quadratic model gives reliable predictions of RTME yield.

In general, the model with p value < .05 is considered to be statistically significant [15]. Based on this, the quadratic term for methanol to oil molar ratio is (x_1x_1), followed by the quadratic term for reaction time (x_4x_4), the linear term for methanol to oil molar ratio (x_1), the linear term for reaction time (x_4), the quadratic term for KOH catalyst concentration (x_2x_2) the linear term for KOH catalyst concentration and reaction time (x_2x_4), and the product term for methanol to oil molar ratio and reaction time (x_1x_4). These were significant factors for infrared radiation-assisted alkaline-catalysed transesterification process which affect RTME yield.

3.3. Optimum process variables for infrared radiation-assisted alkaline-catalysed transesterification

As discussed earlier, RSM was used to optimise the process variables of infrared radiation-assisted alkaline-catalysed transesterification and it was found the optimum methanol to oil molar ratio, KOH catalyst concentration, reaction temperature, and reaction time were 8:1, 1.2 wt%, 64 °C and 68 min respectively. Using the response surface quadratic model (Eq. (4)), the predicted RTME yield was 98.39% with the optimum process variables. The results were similar to those of Holilah et al. [15]. In order to validate the response surface quadratic model and verify the reliability of predictions, the infrared radiation-assisted alkaline-catalysed transesterification was undertaken on a laboratory scale to produce RTME using process variables optimised by RSM. The experiments were conducted in triplicate and it was found average RTME yield was 97.78%, close to the RTME yield (98.39%), predicted using the response surface quadratic model. The result showed higher yield compared with those of Holilah et al. [15] who recorded 95.17% and Sarifah Nurjanah et al. [16] who obtained 61.1%.

Table 2
Box-Behnken experimental design for infrared radiation-assisted alkaline-catalysed transesterification process.

Experimental run no.	Methanol to oil molar ratio	KOH catalyst concentration (wt%)	Reaction temperature (°C)	Reaction time (min)	Experimental RTME yield (%)	Predicted RTME yield (%)
1	8:1	1.5	55	60	92.48	90.43
2	8:1	0.5	60	90	88.79	87.55
3	10:1	0.5	60	60	80.42	80.62
4	8:1	0.5	65	60	92.21	92.83
5	8:1	1.5	60	90	86.01	87.84
6	8:1	1.5	60	30	70.84	73.41
7	8:1	1.0	65	30	75.49	75.04
8	8:1	1.0	60	60	93.12	93.45
9	6:1	1.0	55	60	70.02	69.97
10	10:1	1.0	60	30	63.31	62.07
11	8:1	1.0	60	60	95.32	93.45
12	6:1	0.5	60	60	64.45	66.73
13	8:1	1.0	60	60	93.27	93.45
14	6:1	1.0	65	60	74.69	74.79
15	8:1	1.0	60	60	93.43	93.45
16	6:1	1.0	60	30	54.23	52.19
17	8:1	1.0	55	90	86.21	86.77
18	10:1	1.0	55	60	79.29	80.52
19	6:1	1.5	60	60	72.57	72.48
20	10:1	1.0	60	90	85.49	86.10
21	6:1	1.0	60	90	68.26	68.07
22	8:1	1.5	65	60	95.41	95.33
23	8:1	1.0	60	60	92.11	93.45
24	10:1	1.0	65	60	90.76	92.14
25	10:1	1.5	60	60	88.68	86.50
26	8:1	0.5	60	30	62.58	62.08
27	8:1	1.0	65	90	95.72	94.16
28	8:1	0.5	55	60	82.65	81.30
29	8:1	1.0	55	30	64.32	65.99

Table 3
ANOVA results for response surface quadratic model used to predict RTME yield.

Source	Sum of squares	Degree of freedom	Mean square	F-value	p-value	Prob. > F
Model	4154.59	14	296.76	84.89	<0.0001	Significant
x_1	584.23	1	584.23	167.12	<0.0001	—
x_2	101.44	1	101.44	29.02	<0.0001	—
x_3	202.62	1	202.62	57.96	<0.0001	—
x_4	1194.21	1	1194.21	341.62	<0.0001	—
x_1x_2	4.900 (10^{-3})	1	4.900 (10^{-3})	1.402 (10^{-3})	0.9707	—
x_1x_3	11.56	1	11.56	3.31	0.0904	—
x_1x_4	16.61	1	16.61	4.75	0.0469	—
x_2x_3	10.99	1	10.99	3.14	0.0980	—
x_2x_4	30.47	1	30.47	8.72	0.0105	—
x_3x_4	0.69	1	0.69	0.20	0.6639	—
x_1^2	1224.64	1	1224.64	350.32	<0.0001	—
x_2^2	63.36	1	63.36	18.13	0.0008	—
x_3^2	0.82	1	0.82	0.23	0.6358	—
x_4^2	1030.68	1	1030.68	294.84	<0.0001	—
Residual	48.94	14	3.50			—
Lack of fit	43.51	10	4.35	3.20	0.1366	Not significant
Pure error	5.43	4	1.36			—
Correlated total sum of squares	4203.53	28	—	—	—	—
R^2	0.9884	—	—	—	—	—
Adjusted R^2	0.9767	—	—	—	—	—
Coefficient of variation	2.31	—	—	—	—	—

It can be deduced the use of infrared radiation facilitates the conversion of free fatty acids into methyl ester [18,19]. The quantum energy of infrared photons (0.001–1.7 eV) matches the range of energies separating the quantum states of molecular vibrations. Hence, infrared radiation is capable of penetrating deeper through the reaction mass compared with visible radiation. In addition, infrared radiation is more intensely absorbed compared with microwaves and conventional thermal energy [19,25]. Infrared radiation interacts with the molecules, setting them into vibrational mode, resulting in severe molecular collisions. This increases transfer of thermal energy into reactant molecules which

significantly enhances activation of the reactive species compared with conventional heating systems [26]. Hence, it can be concluded that infrared radiation-assisted alkaline-catalysed transesterification process is an efficient and feasible mean for biodiesel production, and the biodiesel yield can be further increased using optimum process variables.

3.4. Interaction effects of infrared radiation-assisted alkaline-catalysed transesterification process variables on RTME yield

Three-dimensional response surface plots were plotted to

examine the interaction effects of the process variables (methanol to oil molar ratio, KOH catalyst concentration, reaction temperature, and reaction time) on the RTME yield. These plots enabled one to visualise which process variables have a more pronounced effect on RTME yield.

3.4.1. Effect of methanol to oil molar ratio and reaction time

Fig. 3 shows the methanol to oil molar ratio (6:1–10:1) and reaction time (30–90 min) on the RTME yield. Observation shows methanol to oil molar ratio of 8:1 results in the highest RTME yield. However, increasing the methanol to oil molar ratio beyond 8:1 decreases the conversion of free fatty acids into methyl ester, which is due to the reversible characteristics of the transesterification reaction [27] and diffusion of the reaction mixture [28]. In addition, the difference in concentration at the interphase of the RTO and methanol to oil molar ratio creates a driving force, which accelerates mass transfer rate and increases the RTME yield. It has also been proven in another study [29] that increasing the methanol to oil molar ratio beyond 8:1 does not have a significant effect on biodiesel yield. It can also be observed from Fig. 6 that RTME yield is maximised when the reaction time is 68 min. It is apparent from the plot that both the methanol to oil molar ratio and reaction time significantly affect RTME yield (the RTME yield is maximum within the red region of the response surface).

3.4.2. Effect of KOH catalyst concentration and methanol to oil molar ratio

Fig. 4 shows the effect of KOH catalyst concentration (0.5–1.5 wt %) on methanol to oil molar ratio (6:1–10:1) on RTME yield. It can be seen that RTME yield increases slightly when KOH catalyst concentration increases from 0.5 to 1.2 wt%, indicating the RTME yield can only be increased up to a certain level by tweaking KOH catalyst concentration. It is believed RTME yield decreases above a KOH catalyst concentration of 1.2 wt% due to saponification. The results are in line with those of Holilah et al. [15], where RTME yield is maximum when the KOH catalyst concentration is 1.0 wt%. However, they used conventional alkaline-catalysed transesterification (without infrared radiation) for biodiesel production. In addition, it can be observed from Fig. 4 that methanol to oil molar ratio has a more pronounced effect on the RTME yield compared with KOH catalyst concentration. The RTME yield is maximum when the methanol to oil molar ratio is 8:1.

3.4.3. Effect of reaction time and KOH catalyst concentration

Fig. 5 shows the effect of reaction time (30–90 min) and KOH catalyst concentration (0.5–1.5 wt%) on RTME yield. Reaction time

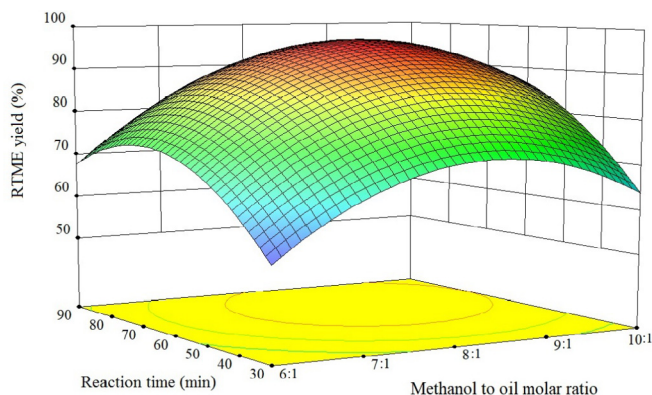


Fig. 3. Response surface plot showing the effect of methanol to oil molar ratio and reaction time on RTME yield.

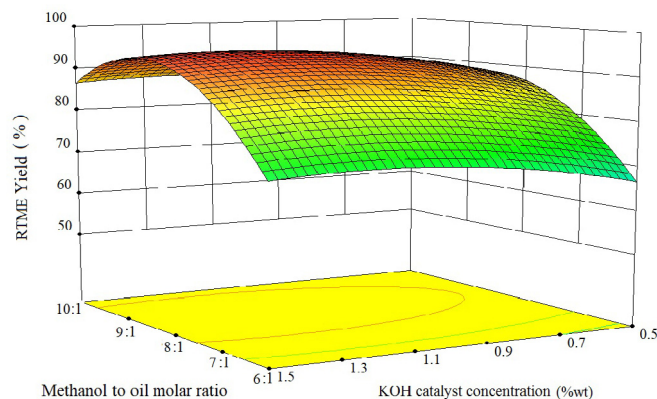


Fig. 4. Response surface plot showing effects of KOH catalyst concentration and methanol to oil molar ratio on the RTME yield.

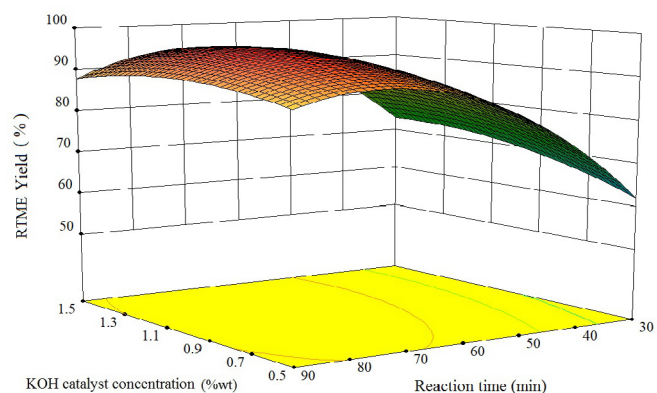


Fig. 5. Response surface plot showing the effect of reaction time and KOH catalyst concentration on RTME yield.

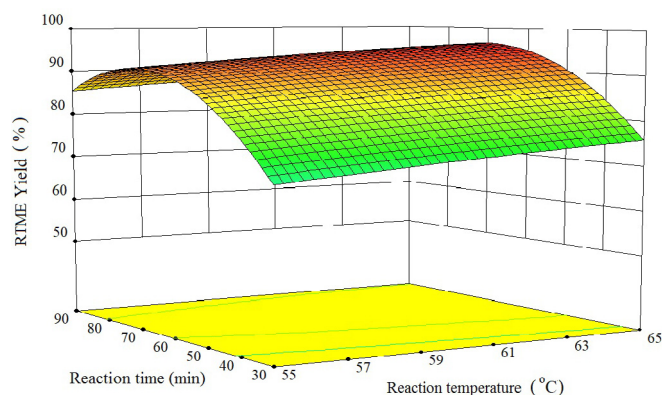


Fig. 6. Response surface plot showing effects of reaction temperature and reaction time on RTME yield.

is one of the factors that can accelerate or decelerate the transesterification reaction and indeed, it can be seen that the RTME yield increases when the reaction time increases from 0 to 68 min, followed by a gradual decrease thereafter. It is believed the use of an infrared lamp during the alkaline-catalysed transesterification process increases thermal energy of the reactants at the start of the transesterification reaction, which promotes RTME production [19,30]. It is evident from Fig. 5 the reaction time has a more significant impact on RTME yield compared with KOH catalyst

concentration, judging from the steepness of the response surface.

3.4.4. Effect of reaction temperature and reaction time

Based on the Pareto chart (Fig. 6), the reaction temperature does not have a significant effect on RTME yield as indicated by its *t*-value (0.55), which is less than the critical *t*-value (2.48). However, it is important to visualise how the reaction temperature affects RTME yield and this is shown in Fig. 6. It can be observed the RTME yield increases slightly when the reaction temperature increases from 55 to 65 °C. The variation in RTME yield is small, indicated by green region of the response surface. The slight increase in RTME yield is likely due to the use of infrared radiation during the alkaline-catalysed transesterification process, which penetrates through the mass of the reactants and excites the molecules of the reactants [19], rather than the reaction temperature. This confirms the reaction temperature does not have a pronounced effect on RTME yield, unlike the reaction time where the RTME yield reaches its maximum value at a reaction time of 68 min.

3.5. Physicochemical properties and FAME content of RTME produced from infrared radiation-assisted alkaline-catalysed transesterification with optimum process variables

The physicochemical properties (kinematic viscosity at 40 °C, density at 15 °C, flash point, calorific value, acid value, and oxidation stability at 110 °C) of the RTME prepared under optimum transesterification process conditions were measured based on ASTM D6751 and EN 14214 standards and the results are summarised in Table 4.

The kinematic viscosity of the RTME is found to be 4.095 mm²/s, which is well within the range specified in the ASTM D6751 standard (1.900–6.000 mm²/s) and EN 14214 standard (3.500–5.000 mm²/s). Holilah et al. [16] reported viscosity of RTME at 6.7 mm²/s was higher compared with the current findings as the oil was processed into biodiesel without purification. Crude oil is required to remove the gum which contains phosphate, protein, carbohydrate, water residue and resin. Therefore, the degumming process can remove the gum and improve the final product [30]. Kumar et al. [3] filtered the crude oil prior to the transesterification process and found that viscosity of biodiesel was reduced to 5.80 mm²/s. Density is also an important parameter of biodiesel because this property will affect the performance of fuel injection systems. The density of the RTME is still well within the range of densities specified in the EN 14214 standard (860.0–900.0 kg/m³). Interestingly, the density of the RTME produced in this study was slightly lower than that of Holilah et al. [16], indicating the infrared radiation-assisted alkaline-catalysed transesterification with optimum process variables does have a positive effect on the density of RTME.

In this study, the acid value of RTME was 0.390 mg KOH/g, which is desirable because it is lower than the maximum permissible limit of acid value specified in the ASTM D6751 and EN 14214 standards

(0.500 mg KOH/g) [25]. The flash point of RTME was 140.0 °C, well within the minimum range specified in the ASTM D6751 standard (100.0–170.0 °C) and the flash point was slightly higher than the minimum limit specified in the EN 14214 standard (120.0 °C), as shown in Table 4. In addition, the oxidation stability of the RTME at 110 °C took about 10.2 h, which may be due to the higher saturated fatty acid chains present in the RTME. The higher oxidation stability of the RTME indicated RTO is a favourable feedstock for biodiesel production. On the whole, the physicochemical properties of RTME produced by infrared radiation-assisted transesterification process are superior compared with those of conventional one.

4. Energy consumption of infrared radiation and water heating bath

Energy consumption of infrared radiation was recorded using infrared reactor and reaction time of 68 min consumed 408 kJ/s as shown in Table 5. The water was heated at 800 W for 20 min for the temperature to reach 60 °C and the time of reaction for a complete transesterification was 90 min. Therefore, the energy consumed to heat the water was 4320 kJ. The preheating time was much longer than the infrared radiation resulting in an increase in energy consumption of biodiesel production. The difference in energy consumptions shows that infrared radiation was more energy efficient than water heating bath. Therefore, infrared radiation assisted method was more energy efficient and produced higher quality biodiesel.

5. Conclusion

The use of non-edible oil to replace fossil-based diesel has been an interesting area of research due to its environmentally friendly qualities. Despite this, technical barriers associated with biodiesel production and usage need to be overcome to increase its quality in addition to introducing efficient methods and increasing the choice of available feedstocks to avoid high cost for large scale production. The intensification process using infrared radiation to produce biodiesel from RTO was aimed at improving the quality of RTME and decrease cost of biodiesel production. There were four process variables of the infrared radiation (methanol to oil molar ratio, KOH catalyst concentration, reaction temperature, and reaction time) optimised using RSM based on the Box-Behnken experimental

Table 5
Energy consumption of infrared radiation and water heating bath.

Parameter	Infrared radiation	Water heating bath
Power (Watt)	100	800
Preheating time (sec)	600	1200
Reaction time (sec)	4080	5400
Energy consumption (kJ)	408	4320

*Energy consumption for 500 mL

*Water heating bath at 1400 Watt by Silitonga et al. [11].

Table 4
Physicochemical properties of RTME produced from infrared radiation-assisted alkaline-catalysed transesterification with optimum process variables.

Property	Unit	Test method [30]	ASTM D6751	EN 14214	Diesel	RTME ^a	RTME ^b
Kinematic viscosity at 40 °C	mm ² /s	ASTM D445	1.9–6.0	3.5–5.0	2.9	4.0	6.7
Density at 15 °C	kg/m ³	ASTM D127	880.0	860.0–900.0	846.1	885.7	887.0
Flash point	°C	ASTM D93	100.0–170.0 (min.)	>120.0	75.5	140.0	148.0
Calorific value	MJ/kg	ASTM D240	–	35,000	45,361	41,140	–
Acid value	mg KOH/g	ASTMD664	0.500 (max.)	0.500 (max.)	0.017	0.390	0.410
Oxidation stability at 110 °C	h	EN 14112	3.0 (min.)	6.0 (min.)	15.2	10.2	–

^a Physicochemical property measured in this study.

^b Physicochemical properties measured by Holilah et al. [15].

design. The optimum methanol to oil molar ratio, KOH catalyst concentration, reaction temperature, and reaction time were 8:1, 1.2 wt%, 64 °C and 68 min respectively, and which resulted in RTME yield of 98.39%. The infrared radiation was conducted in triplicate using the optimum process variables in order to validate the response surface quadratic model. The average RTME yield was found to be 97.78%, close to the predicted value (98.39%), thereby proving the reliability of the model. The results also indicated infrared radiation technique led to reduced time and energy consumption compared with conventional method for biodiesel production. Moreover, the physicochemical properties of the RTME were measured and it was found that the physicochemical properties of the RTME fulfilled the fuel specifications based on the ASTM D6751 and EN 14214 standards. There is a need to examine the engine performance and exhaust emission characteristics of compression ignition engines fuelled with RTME and its blends as well as explore the possibility of producing these fuels on an industrial scale.

Acknowledgments

The authors express their gratitude to Direktorat Jenderal Penguatan Riset dan Pengembangan Kementerian Riset, Teknologi dan Pendidikan Tinggi Republik Indonesia and Politeknik Negeri Medan, Medan, Indonesia. They also acknowledge the financial support provided by the AAIBE Chair of Renewable grant no: 201801 KETHA and Universiti Tenaga Nasional, Malaysia Internal Grant (UNIIG 2017 No. J510050691).

References

- [1] K. Ullah, M. Ahmad, Sofia, F.A. Qureshi, R. Qamar, V.K. Sharma, S. Sultana, M. Zafar, Synthesis and characterization of biodiesel from Amla oil: a promoting non-edible oil source for bioenergy industry, *Fuel Process. Technol.* 133 (2015) 173–182.
- [2] N. Damanik, H.C. Ong, C.W. Tong, T.M.I. Mahlia, A.S. Silitonga, A Review on the Engine Performance and Exhaust Emission Characteristics of Diesel Engines Fueled with Biodiesel Blends, *Environmental Science and Pollution Research*, 2018.
- [3] K.R. Kumar, Channarayappa, K. Chandrika, K.T. Prasanna, B. Gowda, Biodiesel production and characterization from non-edible oil tree species *Aleurites trisperma* Blanco, *Biomass Convers. Bioref.* 5 (2015) 287–294.
- [4] J. Milano, H.C. Ong, H.H. Masjuki, A.S. Silitonga, W.-H. Chen, F. Kusumo, S. Dharma, A.H. Sebayang, Optimization of biodiesel production by microwave irradiation-assisted transesterification for waste cooking oil-*Calophyllum inophyllum* oil via response surface methodology, *Energy Convers. Manag.* 158 (2018) 400–415.
- [5] M. Suresh, C.P. Jawahar, A. Richard, A review on biodiesel production, combustion, performance, and emission characteristics of non-edible oils in variable compression ratio diesel engine using biodiesel and its blends, *Renew. Sustain. Energy Rev.* 92 (2018) 38–49.
- [6] J. Milano, H.C. Ong, H.H. Masjuki, W.T. Chong, M.K. Lam, P.K. Loh, V. Vellayan, Microalgae biofuels as an alternative to fossil fuel for power generation, *Renew. Sustain. Energy Rev.* 58 (2016) 180–197.
- [7] A.K. Azad, M.G. Rasul, M.M.K. Khan, S.C. Sharma, M. Mofijur, M.M.K. Bhuiya, Prospects, feedstocks and challenges of biodiesel production from beauty leaf oil and castor oil: a nonedible oil sources in Australia, *Renew. Sustain. Energy Rev.* 61 (2016) 302–318.
- [8] K. Noiroj, P. Intarapong, A. Luengnaruemitchai, S. Jai-In, A comparative study of KOH/Al₂O₃ and KOH/NaY catalysts for biodiesel production via transesterification from palm oil, *Renew. Energy* 34 (2009) 1145–1150.
- [9] G. Knothe, L.F. Razon, Biodiesel fuels, *Prog. Energy Combust. Sci.* 58 (2017) 36–59.
- [10] A.K. Agarwal, A. Shrivastava, R.K. Prasad, Evaluation of toxic potential of particulates emitted from *Jatropha* biodiesel fuelled engine, *Renew. Energy* 99 (2016) 564–572.
- [11] A.S. Silitonga, T.M.I. Mahlia, H.C. Ong, T.M.I. Riayatsyah, F. Kusumo, H. Ibrahim, S. Dharma, D. Gumilang, A comparative study of biodiesel production methods for *Reutealis trisperma* biodiesel, *Energy Sources, Part A Recovery, Util. Environ. Eff.* 39 (2017) 2006–2014.
- [12] C. Martín, A. Moure, G. Martín, E. Carrillo, H. Domínguez, J.C. Parajó, Fractional characterisation of *Jatropha*, neem, moringa, *trisperma*, castor and candlenut seeds as potential feedstocks for biodiesel production in Cuba, *Biomass Bioenergy* 34 (2010) 533–538.
- [13] E. Ramayeni, B.H. Susanto, D.F. Pratama, Synthesis of kemiri sunan (*reutealis trisperma* (blanco) airy shaw) H-FAME through partially hydrogenation using Ni/C catalyst to increase oxidation stability, *Earth Environ. Sci.* 105 (2018) 1–6.
- [14] T.M.I. Riayatsyah, H.C. Ong, W.T. Chong, L. Aditya, Heri Hermansyah, T.M.I. Mahlia, Life cycle cost and sensitivity analysis of *Reutealis trisperma* as non-edible feedstock for future biodiesel production, *Energies* 10 (2017) 877.
- [15] H. Holilah, D. Prasetyoko, T.P. Oetami, E.B. Santosa, Y.M. Zein, H. Bahruji, H. Fansuri, R. Ediati, J. Juwari, The potential of *Reutealis trisperma* seed as a new non-edible source for biodiesel production, *Biomass Convers. Bioref.* 5 (2015) 347–353.
- [16] D.S.L. Sarifah Nurjanah, Asri Widyasanti, Sudaryanto Zain, The effect of NaOH concentration and length of transesterification time on characteristic of FAME from *Reutealis trisperma* (kemiri sunan), *Int. J. Adv. Sci. Eng. Inf. Technol.* 5 (2015) 52–56.
- [17] C. Bindhu, J.R.C. Reddy, B.V.S.K. Rao, T. Ravinder, P.P. Chakrabarti, M.S.L. Karuna, R.B.N. Prasad, Preparation and evaluation of biodiesel from *Sterculia foetida* seed oil, *J. Am. Oil Chem. Soc.* 89 (2012) 891–896.
- [18] F. Kusumo, A.S. Silitonga, H.C. Ong, H.H. Masjuki, T.M.I. Mahlia, A Comparative Study of Ultrasound and Infrared Transesterification of *Sterculia foetida* Oil for Biodiesel Production, *Energy Sources, Part A: Recovery, Utilization, and Environmental Effects*, 2017, pp. 1–8.
- [19] R. Chakraborty, H. Sahu, Intensification of biodiesel production from waste goat tallow using infrared radiation: process evaluation through response surface methodology and artificial neural network, *Appl. Energy* 114 (2014) 827–836.
- [20] I. Korkut, M. Bayramoglu, Selection of catalyst and reaction conditions for ultrasound assisted biodiesel production from canola oil, *Renew. Energy* 116 (2018) 543–551.
- [21] I. Choedkiatsakul, K. Ngaosuwan, S. Assabumrungrat, S. Mantegna, G. Cravotto, Biodiesel production in a novel continuous flow microwave reactor, *Renew. Energy* 83 (2015) 25–29.
- [22] P. Pradhan, S. Chakraborty, R. Chakraborty, Optimization of infrared radiated fast and energy-efficient biodiesel production from waste mustard oil catalyzed by Amberlyst 15: engine performance and emission quality assessments, *Fuel* 173 (2016) 60–68.
- [23] S.M.D.A. Alajmi Fnyees, H.A. Aziz, A.N. Mariah, A.L. Chuah, Recent trends in biodiesel production from commonly used animal fats, *Int. J. Energy Res.* 42 (2018) 885–902.
- [24] A. Bokhari, S. Yusup, L.F. Chuah, J.J. Klemeš, S. Asif, B. Ali, M.M. Akbar, R.N.M. Kamil, Pilot scale intensification of rubber seed (*Hevea brasiliensis*) oil via chemical interesterification using hydrodynamic cavitation technology, *Bioresour. Technol.* 242 (2017) 272–282.
- [25] L.F. Chuah, J.J. Klemeš, S. Yusup, A. Bokhari, M.M. Akbar, A review of cleaner intensification technologies in biodiesel production, *J. Clean. Prod.* 146 (2017) 181–193.
- [26] A.D.d. Oliveira, A.F.d. Sá, M.F. Pimentel, J.G.A. Pacheco, C.F. Pereira, M.S. Larrechi, Comprehensive near infrared study of *Jatropha* oil esterification with ethanol for biodiesel production, *Spectrochim. Acta Mol. Biomol. Spectrosc.* 170 (2017) 56–64.
- [27] T.G. Kudre, N. Bhaskar, P.Z. Sakhare, Optimization and characterization of biodiesel production from rohu (*Labeo rohita*) processing waste, *Renew. Energy* 113 (2017) 1408–1418.
- [28] P. Verma, M.P. Sharma, Comparative analysis of effect of methanol and ethanol on Karanja biodiesel production and its optimisation, *Fuel* 180 (2016) 164–174.
- [29] M. Mofijur, A.E. Atabani, H.H. Masjuki, M.A. Kalam, B.M. Masum, A study on the effects of promising edible and non-edible biodiesel feedstocks on engine performance and emissions production: a comparative evaluation, *Renew. Sustain. Energy Rev.* 23 (2013) 391–404.
- [30] H.C. Ong, H.H. Masjuki, T.M.I. Mahlia, A.S. Silitonga, W.T. Chong, K.Y. Leong, Optimization of biodiesel production and engine performance from high free fatty acid *Calophyllum inophyllum* oil in CI diesel engine, *Energy Convers. Manag.* 81 (2014) 30–40.